

Supplemental methods

Liver enzyme analysis

Sera alanine aminotransferase (ALT) and aspartate transaminase (AST) levels were measured by Queensland Pathology using a Beckman Unicell DxC800 analyzer.

Histology

Mouse livers were fixed in 10% neutral-buffered formalin and processed as previously described (Liu, Blake et al. 2016). Hematoxylin and eosin (H&E) staining was performed by QIMR Berghofer histology facility. H&E-stained tissue sections were imaged using Aperio Scanscope AT (Leica) and analyzed by Aperio ImageScope.

Serum cytokine measurement

Mouse blood was collected, allowed to clot, and centrifuged at 10,000 rpm for 10 min to separate sera. Cytokine levels were determined using mouse cytometric bead array (CBA) as per manufacturer's instructions (BD Biosciences).

Immune checkpoint blockade

Anti-PD-1 mAbs (rat IgG2a, RMP1-14, BioxCel) and anti-CTLA-4 mAbs (mouse IgG2a, 9D9, Bristol-Myers Squibb) were administered i.p. twice a week at the dose of 100 ug and 200 ug respectively.

***In silico* model for MM cells - CD8⁺ T cell interactions**

Modeling was performed using the MATLAB software. We started from the model recently proposed by Doban et al. which captures the effect of the tumor cells on the immune system and vice-versa through predator-prey competition terms (Doban and Lazar 2017). In addition to the three populations proposed by Doban et al. (tumor cells, i.e. myeloma; hunting immune cells, i.e. activated CD8⁺ T cells; and resting immune cells, i.e. naïve CD8⁺ T cells), we introduced a fourth population of exhausted CD8⁺ T cells. We used the Gompertz model (Enderling and Chaplain 2014) for MM and CD8⁺ T cell growth. Moreover, we used delay differential equations to take into account time delays in CD8⁺ T cell activation, CD8⁺ T cell contraction after activation as well as tumor dormancy.

We used the following equations:

$\forall M, A, Z, E \in \mathbb{R}^+$,

$$\frac{dM}{dt} = R_M \min(M, M_{(t-10)}) \log\left(\frac{K_M}{M}\right) - \gamma A_{(t-1)} = f(M, A)$$

$$\begin{aligned} \frac{dA}{dt} = & R_A \min(A, A_{(t-1)}) \log\left(\frac{K_{AZE} - Z - E}{A}\right) + \beta_S Z \log\left(\frac{\lambda_A K_{AZE} + 1}{A}\right) \\ & + \beta_T \log(\min(M_{(t-2)}, M)) Z \log\left(\frac{\lambda_A K_{AZE} + 1}{A}\right) f(M, A) + \beta_A Z \log\left(\frac{\lambda_A K_{AZE} + 1}{A}\right) \\ & - \rho(\min(A, A_{(t-2)})) \exp\left(\frac{-M_{(t-3)}}{c}\right) - \sigma_A \min(A, A_{(t-1)}) \sqrt{\frac{\min(M, M_{(t-2)})}{\alpha_A}}, \end{aligned}$$

if $f(M, A) \geq 0$

$$\begin{aligned} \frac{dA}{dt} = & R_A \min(A, A_{(t-1)}) \log\left(\frac{K_{AZE} - Z - E}{A}\right) + \beta_S Z \log\left(\frac{\lambda_A K_{AZE} + 1}{A}\right) + \beta_A Z \log\left(\frac{\lambda_A K_{AZE} + 1}{A}\right) \\ & - \rho(\min(A, A_{(t-2)})) \exp\left(\frac{-M_{(t-3)}}{c}\right) - \sigma_A \min(A, A_{(t-1)}) \sqrt{\frac{\min(M, M_{(t-2)})}{\alpha_A}}, \end{aligned}$$

if $f(M, A) < 0$

$$\begin{aligned} \frac{dZ}{dt} = & R_Z Z \log\left(\frac{K_{AZE} - A - E}{Z}\right) - \beta_S Z \log\left(\frac{\lambda_A K_{AZE} + 1}{A}\right) \\ & - \beta_T \log(\min(M_{(t-2)}, M)) Z \log\left(\frac{\lambda_A K_{AZE} + 1}{A}\right) f(M, A) - \beta_A Z \log\left(\frac{\lambda_A K_{AZE} + 1}{A}\right) \\ & - \sigma_Z Z \sqrt{\frac{\min(M, M_{(t-2)})}{\alpha_Z}}, \quad f(M, A) \geq 0 \end{aligned}$$

$$\begin{aligned} \frac{dZ}{dt} = & R_Z Z \log\left(\frac{K_{AZE} - A - E}{Z}\right) - \beta_S Z \log\left(\frac{\lambda_A K_{AZE} + 1}{A}\right) - \beta_A Z \log\left(\frac{\lambda_A K_{AZE} + 1}{A}\right) - \sigma_Z Z \sqrt{\frac{\min(M, M_{(t-2)})}{\alpha_Z}}, \\ & f(M, A) < 0 \end{aligned}$$

$$\frac{dE}{dt} = \sigma_A \min(A, A_{(t-1)}) \sqrt{\frac{\min(M, M_{(t-2)})}{\alpha_A}} - \theta E_{(t-5)}$$

M represents the MM cell population; A are activated CD8⁺ T cells, Z, naïve CD8⁺ T cells and E, exhausted CD8⁺ T cells. $\frac{dM}{dt}$, $\frac{dA}{dt}$, $\frac{dZ}{dt}$ and $\frac{dE}{dt}$ refer to their respective derivatives. Log is the natural

logarithm. $X_{(t-x)}$ refers to the value of the variable X at the time $t - x$. $\min(x, y)$ refers to the minimal value between x and y . R_M , R_A , R_Z are the growth rates of MM cells, activated CD8⁺ T cells and naïve CD8⁺ T cells respectively. The system is bounded due to the physical constraint of the BM and K_M and K_{AZE} are the maximal carrying capacities for MM cells, and total CD8⁺ T cells respectively. λ_A is the maximal proportion of activated CD8⁺ T cells within total CD8⁺ T cells. γ is the MM cell-killing capacity of activated CD8⁺ T cells. β_S is the conversion rate of naïve CD8⁺ T cells into activated CD8⁺ T cells at steady state, β_T is the conversion rate in the presence of tumor and β_A is the conversion rate induced by anti-CD137 mAb treatment. ρ is the contraction rate of CD8⁺ T cells after activation, this contraction is slowed down in the presence of tumor and c modulates the tumor-dependent delay in contraction. σ_Z and σ_A refer to the suppressive effect of the tumor on resting and activated CD8⁺ T cells, respectively; and α_Z and α_A were introduced to adjust the negative effect of the tumor. θ is the death rate of exhausted cells.

MM cell numbers are determined by the difference between MM cell growth and MM cell killing by activated CD8⁺ T cells. Activated CD8⁺ T cell numbers vary accordingly to the growth of existing activated cells, the conversion from naïve cells into activated CD8⁺ T cells, the contraction of activated CD8⁺ T cells and MM suppressive effect. Similarly, naïve CD8⁺ T cell numbers are function of the growth of naïve CD8⁺ T cells (since naïve CD8⁺ T cells are not proliferative, this term reflects the arrival of new naïve CD8⁺ T cells into the BM), their conversion into activated CD8⁺ T cells and MM suppressive effect. We introduced different types of conversion: naïve CD8⁺ T cells become activated at a very low rate in steady state conditions (to reproduce the small percentage of activated cells observed in naïve mice) and this is controlled by the factor β_S ; then naïve CD8⁺ T cells convert into activated cells as a result of tumor sensing, this is controlled by the factor β_T ; and finally naïve cells become activated as a result of the anti-CD137 mAb treatment, this is controlled by the factor β_A . Suppression of activated CD8⁺ T cells by the MM cells gives rise to exhausted cells that do not proliferate and are no longer able to kill MM cells. The number of exhausted CD8⁺ T cells is the difference between exhausted CD8⁺ T cells generated as a result of tumor-suppression and the death of exhausted CD8⁺ T cells.

To model the time it takes for the tumor to seed the BM, for adaptive immune responses to develop and for T cells to contract after activation, we introduced time delays. Time delays were as followed: 10 days for tumor dormancy (reproduces the delay in MM growth observed after MM cell injection), 3

days for tumor sensing by the immune system (corresponds to the time needed for antigen presenting cell activation and antigen processing for presentation to naïve CD8⁺ T cells), 1 day for CD8⁺ T cell activation (correspond to the time when naïve CD8⁺ T cells interact with antigen presenting cells and become fully activated), 2 days before activated CD8⁺ T cells start to contract. This contraction is delayed if activated CD8⁺ T cells are still stimulated i.e. MM cells are still present or have been present in the 3 preceding days. Finally, there is a delay of 2 days before MM cells start to have a negative effect on CD8⁺ T cells (reflects our experimental observations that CD8 T cells are only decreased at late time points) and a delay of 10 days before exhausted CD8⁺ T cells start to die.

From our experimental observations, the femur of a naïve mouse contains an average of 1.4×10^5 total CD8⁺ T cells, and approximately 10 % of them are activated (considering that IFN γ ⁺ cells are functionally activated cells). The maximum value of total CD8⁺ T cells measured in our experiments was 8.6×10^5 and activated CD8⁺ T cells represented up to 90 % of this population (values obtained following anti-CD137 mAb treatment), thus $\lambda_A = 0.9$. We then determined β_s (conversion rate of naïve CD8 T cells into activated CD8 T cells at steady state) and ρ (contraction rate of CD8 T cells after activation) as well as R_Z and R_A (respective growth rates of naïve and activated CD8 T cells) so the numbers of naïve and activated CD8 T cells remained stable in the absence of tumor (Supplemental Figure 11A).

We then determined the optimal parameters for tumor growth in untreated mice (Supplemental Table 1). While keeping the other parameters constant at their optimal values, we tested different initial numbers of myeloma cells and found that this number had to be greater than 19 295 myeloma cells for the tumor to grow (Supplemental Figure 11B). Of note, although the outcome was completely different between 19294 and 19295 initial MM cells, the tumor growth curves were very similar with 20 000 cells or 25 000 initial MM cells, indicating a threshold effect. This threshold effect might explain why some mice injected with Vk*MYC cells never developed the tumor (generally 5-10% of the mice in our experimental settings). We chose the fitted initial MM cell numbers to be 21 000. This corresponds to 1.05 % of the 2×10^6 cells we injected in our experiments. While this percentage may appear low, we have to consider that the cells injected are whole splenocytes from a *Rag2^{-/-}Il2 γ 2^{-/-}* mouse 5 weeks after injection of Vk*MYC cells and contain approximately 50 % MM cells (this may vary with different batches of cells obtained from different *Rag2^{-/-}Il2 γ 2^{-/-}* spleens). Moreover, not all MM cells injected reach the BM and our calculations are based on a small portion of the whole BM (1

femur). In reason of the 10 days delay in MM cell growth representing tumor seeding and dormancy, MM cell numbers initially decreased due to CD8 T cell-mediated killing (Supplemental Figure 11C). However, by day 10, MM cell numbers started to increase. This increase was initially slow and MM cell numbers remain below 1.5×10^5 until day 20 (Figure 8A), in agreement with our experimental observations with the Vk12653 Vk*MYC cell line. While keeping the other parameters constant at their optimized values, the minimal tumor growth rate and the maximal killing capacity of activated CD8⁺ T cells allowing the tumor to grow were respectively $R_M = 0.18$ and $\gamma = 0.088$ (Supplemental Figures 11D and E). The minimal suppressive effect on activated CD8⁺ T cells allowing the tumor to grow was $\sigma_A = 0.03$ (Figure 11F). Interestingly, tumor was able to grow even when it did not suppressed naïve CD8 T cells i.e. $\sigma_Z = 0$ (Data not shown).

Having set up the optimal parameters in untreated conditions, we then considered the effect of anti-CD137 mAb treatment. CD137 stimulation is known to induce CD8⁺ T cell activation and proliferation, increase their cytotoxic activity and promote their survival (Makkouk, Chester et al. 2016). Therefore, we hypothesized that the following parameters would be modified by the treatment: the conversion of naïve CD8⁺ T cells into activated CD8⁺ T cells (β_A) as well as the growth rate of activated CD8⁺ T cells (R_A) and their killing capacity (γ) increase while their contraction rate (ρ) will decrease. In our experiments, treatment was given twice a week for two weeks. For instance, if the treatment was started on day 14, mice received injections of anti-CD137 mAbs on days 14, 17, 21 and 24. The half-life of anti-CD137 mAbs used in our experiments is 7 days (Foell, Strahotin et al. 2003) therefore we supposed that the effect of the treatment will last 7 days after the last injection (i.e. for a treatment starting on day 14, the effect of the treatment will stop on day 31). We tested the effect of the treatment in the absence of tumor using the fitted parameters shown in Supplemental Table 1 and confirmed that it induced a transient expansion of activated CD8⁺ T cells (Supplemental Figure 8B).

	Parameter	Biological meaning	Fitted value
Constant	Initial number of MM cells	Number of live MM cells reaching 1 femur	21 000
	R_M	Growth rate of MM cells	0.35
	R_Z	Growth rate of naïve CD8 ⁺ T cells	0.005
	K_M	MM carrying capacity	5×10^6
	K_{AZE}	Total CD8 ⁺ T cell carrying capacity	9×10^5
	β_S	Steady state conversion rate of naïve CD8 ⁺ T cells into activated CD8 ⁺ T cells	0.00238061
	β_T	Tumor-induced conversion rate of naïve CD8 ⁺ T cells into activated CD8 ⁺ T cells	5×10^{-9}
	c	Modulates the tumor-depend delay in contraction	5000
	σ_Z	Negative effect of the tumor on naïve CD8 ⁺ T cells	0.01
	σ_A	Negative effect of the tumor on activated CD8 ⁺ T cells	0.05
	α_Z	Modulates the negative effect of the tumor on naïve CD8 ⁺ T cells	5000
α_A	Modulates the negative effect of the tumor on activated CD8 ⁺ T cells	5000	
Untreated conditions	R_A	Growth rate of activated CD8 ⁺ T cells	0.08
	β_A	Treatment-induced conversion rate of naïve CD8 ⁺ T cells into activated CD8 ⁺ T cells	0
	ρ	Contraction rate of activated CD8 ⁺ T cells	0.4949
	γ	killing capacity of activated CD8 ⁺ T cells	0.08
Anti-CD137 mAb treatment	R_A	Growth rate of activated CD8 ⁺ T cells	0.15
	β_A	Treatment-induced conversion rate of naïve CD8 ⁺ T cells into activated CD8 ⁺ T cells	0.02
	ρ	Contraction rate of activated CD8 ⁺ T cells	0.000001
	γ	killing capacity of activated CD8 ⁺ T cells	2.7

Supplemental Table 1: Fitted parameters in untreated conditions and during anti-CD137 mAb treatment. The parameters were chosen to best fit the experimental data.

References

Doban, A. I. and M. Lazar (2017). "A switching control law approach for cancer immunotherapy of an evolutionary tumor growth model." Math Biosci **284**: 40-50.

Enderling, H. and M. A. Chaplain (2014). "Mathematical modeling of tumor growth and treatment." Curr Pharm Des **20**(30): 4934-4940.

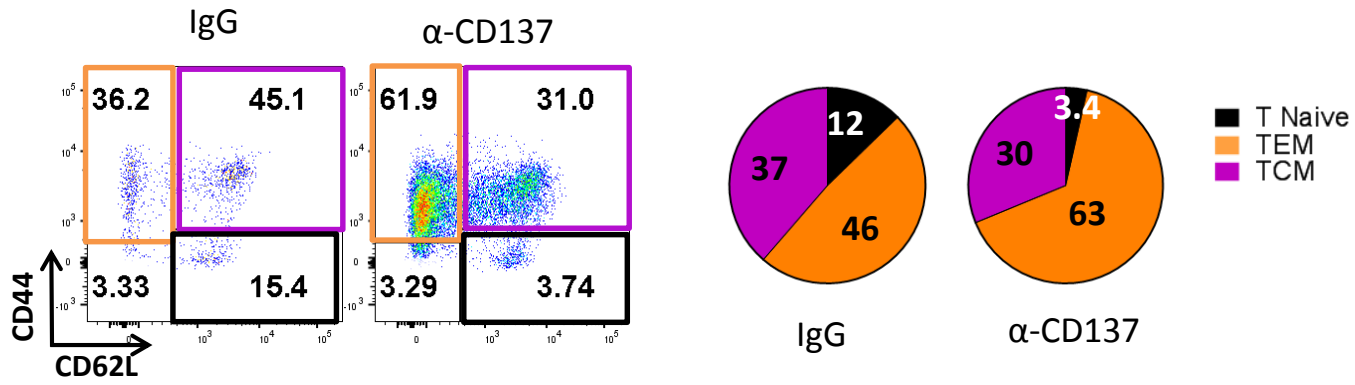
Foell, J., S. Strahotin, S. P. O'Neil, M. M. McCausland, C. Suwyn, M. Haber, P. N. Chander, A. S. Bapat, X. J. Yan, N. Chiorazzi, M. K. Hoffmann and R. S. Mittler (2003). "CD137 costimulatory T cell receptor engagement reverses acute disease in lupus-prone NZB x NZW F1 mice." J Clin Invest **111**(10): 1505-1518.

Liu, J., S. J. Blake, H. Harjunpaa, K. A. Fairfax, M. C. Yong, S. Allen, H. E. Kohrt, K. Takeda, M. J. Smyth and M. W. Teng (2016). "Assessing Immune-Related Adverse Events of Efficacious Combination Immunotherapies in Preclinical Models of Cancer." Cancer Res **76**(18): 5288-5301.

Makkouk, A., C. Chester and H. E. Kohrt (2016). "Rationale for anti-CD137 cancer immunotherapy." Eur J Cancer **54**: 112-119.

-

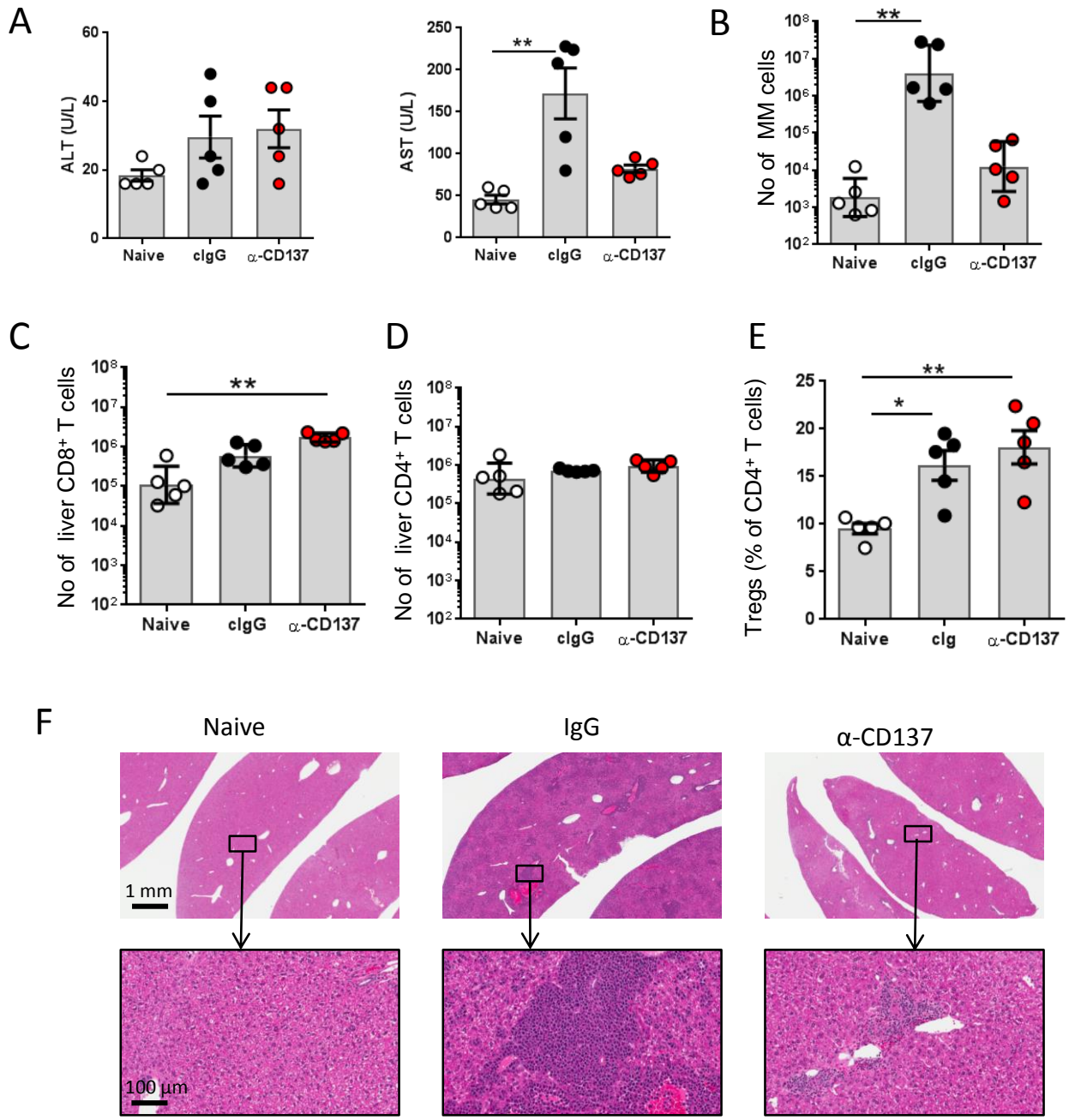
Supplemental Figure 1



Supplemental Figure 1. Treatment with anti-CD137 mAbs increases the effector memory CD8 T cell pool in the BM.

WT mice were challenged with Vk*MYC cells and 3 weeks later, mice received a single ip injection of 100 μ g of anti-CD137 mAbs or control IgG, twice. The memory status of BM CD8⁺ T cell was analyzed by flow cytometry at week 4 post Vk*MYC cell challenge. Naive cells were defined as CD62L⁺CD44⁻, central memory cells (TCM) as CD44⁺CD62L⁺ and effector memory cells (TEM) as CD44⁺CD62L⁻. Representative dot plots (left) and pie-charts displaying mean values (right) for n= 5 mice per groups are shown.

Supplemental Figure 2

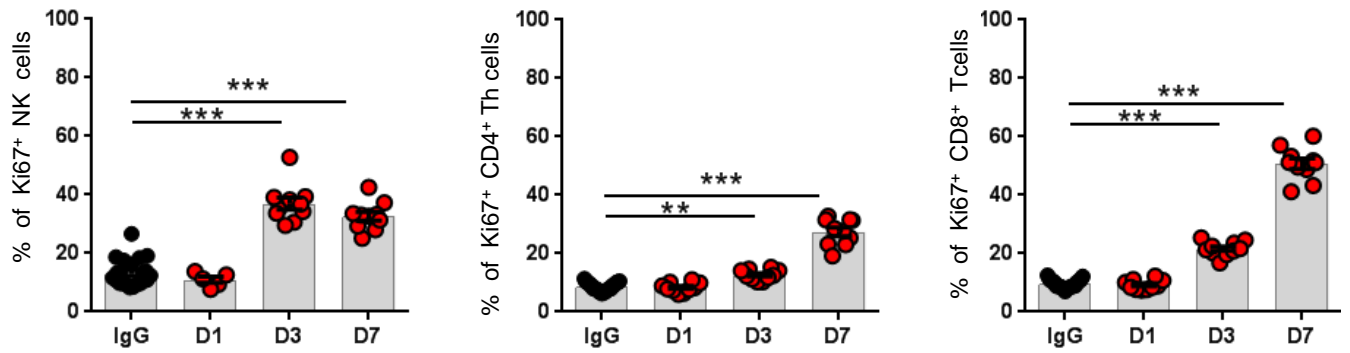


Supplemental Figure 2: Anti-CD137 mAb treatment increases CD8+ T cell liver infiltration with minimal hepatotoxicity.

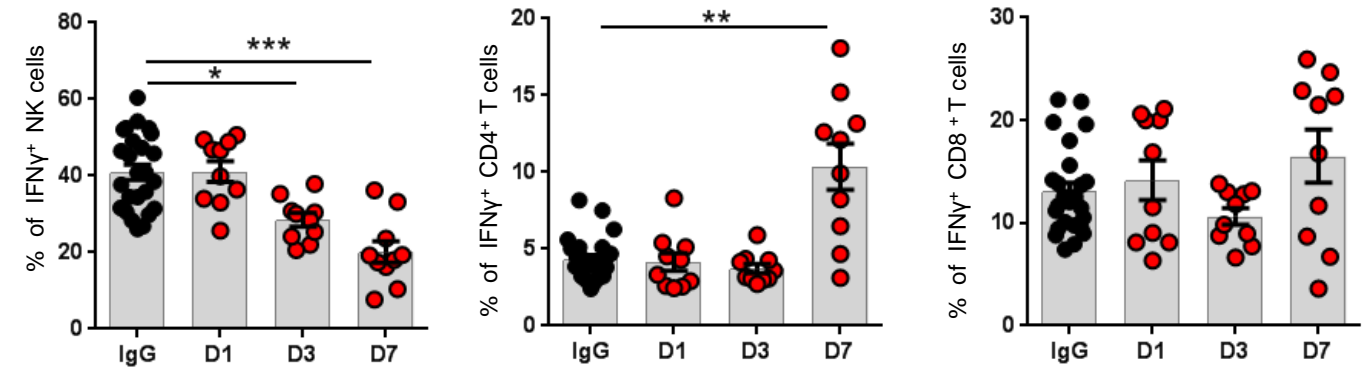
WT mice were challenged with Vk*MYC cells and 2 weeks later, mice received a 2 week-anti-CD137 mAb treatment. Analysis was performed at week 6 post Vk*MYC cell challenge. (A) Serum was collected for the analysis of alanine transaminase (ALT) and aspartate transaminase (AST) levels. (B-F) Livers were collected; the left lateral lobe was fixed in PFA for histology analysis while the rest of the liver was processed for flow cytometry analysis. Numbers of liver-infiltrating (B) MM cells as well as (C) CD8+ and (D) CD4+ T cells and percentages of (E) FoxP3+ Tregs were determined by flow cytometry. Graphs show the (A, E) mean \pm SEM or (B-D) geometric mean \pm SD of 1 experiment with n=5 mice per group. Data were analyzed with a Kruskal-Wallis test followed by a Dunn's multiple comparison post-hoc test. * p < 0.05; ** p < 0.01 (F) Representative haematoxylin and eosin liver staining of n= 5 mice per group. Top panel, scale: 1 mm; lower panel, scale: 100 μ m.

Supplemental Figure 3

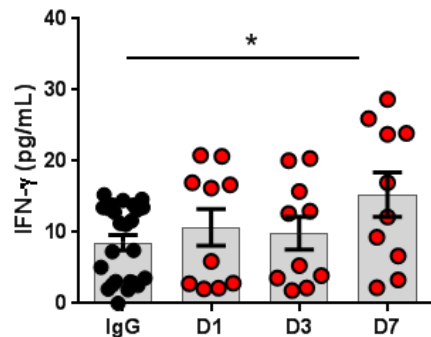
A



B

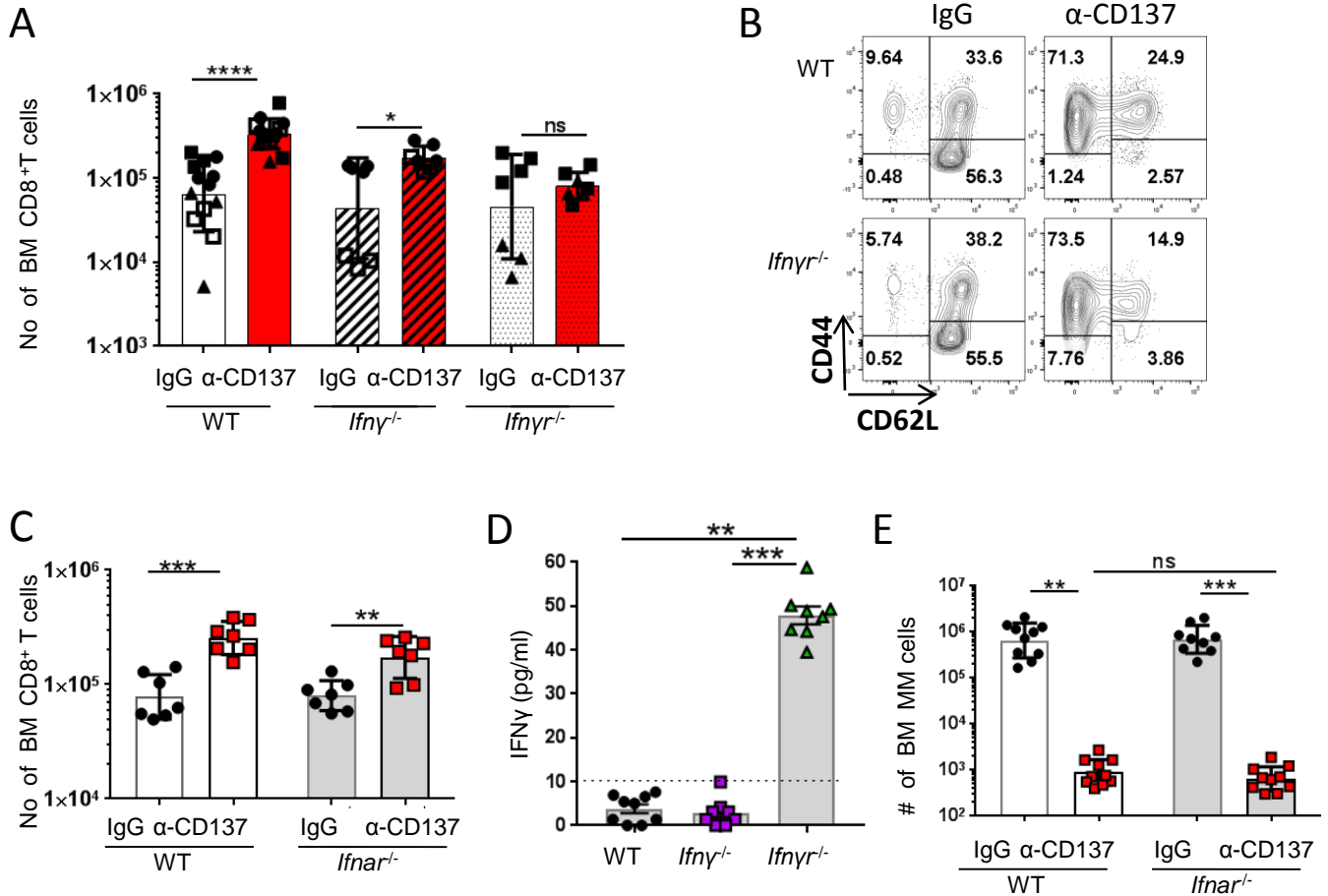


C



Supplemental Figure 3: NK cells and T cells proliferate in the spleen of anti-CD137 mAb-treated mice but produce limited amount of IFN γ . Naïve WT mice received a single ip injection of 100 μ g of anti-CD137 mAbs or control IgG. (A) Percentages of proliferative (Ki67⁺) NK cells, FoxP3⁻ CD4⁺ Th cells and CD8⁺ T cells in the spleen were analyzed by flow cytometry at day 1, 3 and 7 post anti-CD137 mAb injection. (B) Splenocytes were cultured with PMA-ionomycin for 2 hrs and IFN γ production by NK cells, CD4⁺ T cells and CD8⁺ T cells was assessed by intracellular staining at day 1, 3 and 7 post anti-CD137 mAb injection. (C) Serum IFN γ levels were analyzed by Cytometric Bead Array (CBA). Graphs display the mean \pm SEM of data from 2 pooled experiments, with n=5-10 mice per group. Data were analyzed with a Kruskal-Wallis test followed by a Dunn's multiple comparisons post-hoc test. * p < 0.05; ** p < 0.01; *** p < 0.001.

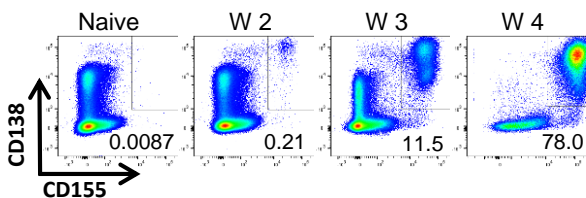
Supplemental Figure 4



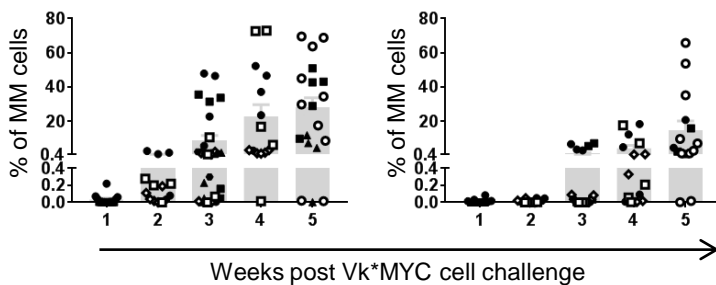
Supplemental Figure 4: Type I IFN are not required for CD8⁺ T cell expansion nor for anti-MM efficacy of anti-CD137 mAbs. (A-C) Naive WT, *Ifnyr*^{-/-}, *Ifnyr*^{-/-} or *Ifnar*^{-/-} mice received a 2-week anti-CD137 mAb treatment. (A) CD8⁺ T cell numbers in the BM of WT, *Ifnyr*^{-/-} and *Ifnyr*^{-/-} mice were determined by flow cytometry. Graphs show the geometric mean ± SD of 4 pooled experiments. Data acquired within the same experiment are depicted with similar symbols. (B) The memory status of BM CD8⁺ T cells of WT and *Ifnyr*^{-/-} mice was determined by flow cytometry. Representative dot plots of 2 experiments with a total of n= 6-7 mice per group are shown. (C) CD8⁺ T cell numbers in the BM of WT and *Ifnar*^{-/-} mice were determined by flow cytometry. Graphs show the geometric mean ± SD of 2 pooled experiments. (D) WT, *Ifnyr*^{-/-} or *Ifnyr*^{-/-} mice were challenged with Vk*MYC cells and after 3 weeks, serum IFN γ levels were determined by cytometric beads array (CBA). Data are shown as mean ± SEM of 1 experiment with n=8-9 mice per group. The dotted line shows the limit of detection. (E) WT or *Ifnar*^{-/-} mice were challenged with Vk*MYC cells and after 2 weeks, they received 3 ip injections of 100 μ g of anti-CD137 mAbs at 3-4 day-intervals. MM cell numbers were determined by flow cytometry at week 5 post Vk*MYC cell challenge. Graphs show the geometric mean ± SD of 1 experiment with n=9-10 mice per group. Data were analyzed with (A, C) a Mann-Whitney U test or (D, E) Kruskal-Wallis test followed by a Dunn's multiple comparisons post-hoc test. * p < 0.05, ** p < 0.01; *** p < 0.001; **** p < 0.0001, ns: non significant.

Supplemental Figure 5

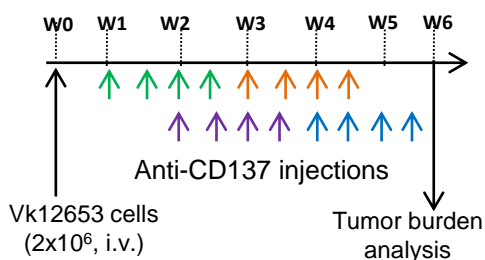
A



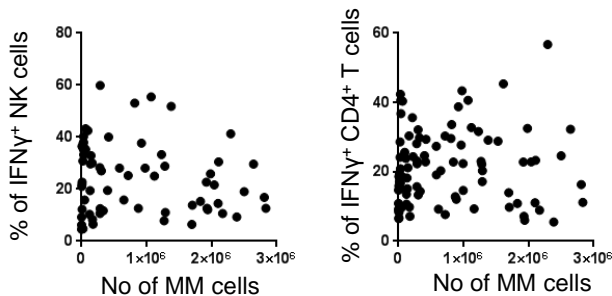
B



C



D

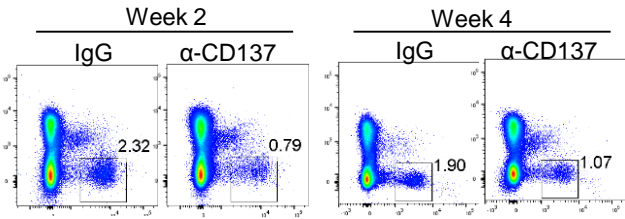


Supplemental Figure 5: MM grows slowly in the BM and spleen of Vk^*MYC cell challenged mice.

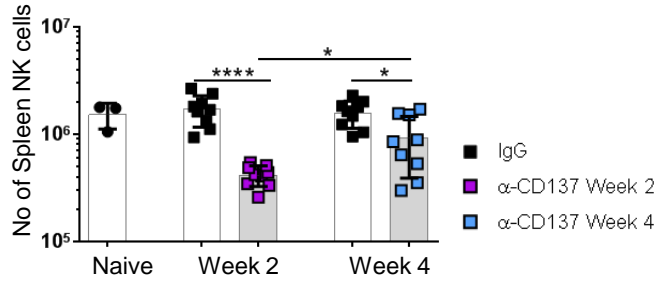
WT mice were challenged with cells. (A) Representative dot-plots showing the percentages of CD155⁺ plasma cells (MM cells) in the BM at week 2, 3 and 4 post Vk^*MYC cell challenge. (B) Quantification of the percentages of MM cells in the BM (left) and spleen (right) at 1, 2, 3, 4 and 5 post $Vk12653$ cell injection. Data are pooled from $n=7$ independent experiments. Each dot represent an individual mouse, data obtained from the same experiment are displayed with the same symbols. (C) Experiment design for the data presented in Figure 5A, B. WT mice were challenged with Vk^*MYC cells and divided into 5 groups. The first 4 groups of mice received a 2-week anti-CD137mAb treatment (4 ip injections of anti-CD137 mAb over a period of 2 weeks; 3-4 days interval between each injection) starting at different time points. Anti-CD137 mAb injections are shown by the arrows on the diagram: week 1 treatment group in green, week 2 treatment group in purple, week 3 treatment group in orange, week 4 treatment group in blue. Another group of mice received control IgG injections twice a week from week 1 to week 6. Tumor burden was analyzed by flow cytometry at week 6. (D) WT mice were challenged with Vk^*MYC cells and 3 to 6 weeks later, BM cells were collected and cultured with PMA-ionomycin for 2 hrs. IFN γ -production by NK cells (right) or CD4⁺ T cells (left) was measured by intracellular staining. Data were pooled from $n=10$ independent experiments with a total of $n=91$ mice that have either been untreated or received control treatment (PBS or IgG). No significant correlation was observed using either linear regression or unconstrained segmental linear regression.

Supplemental Figure 6

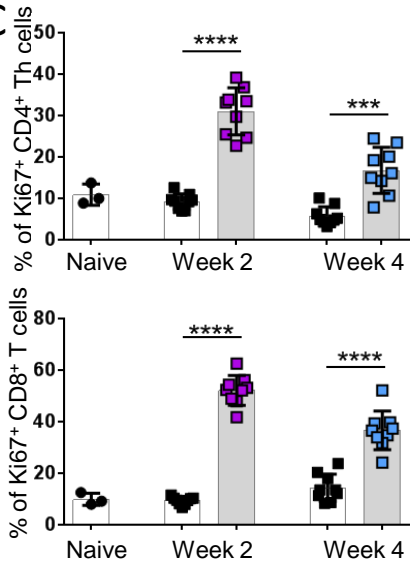
A



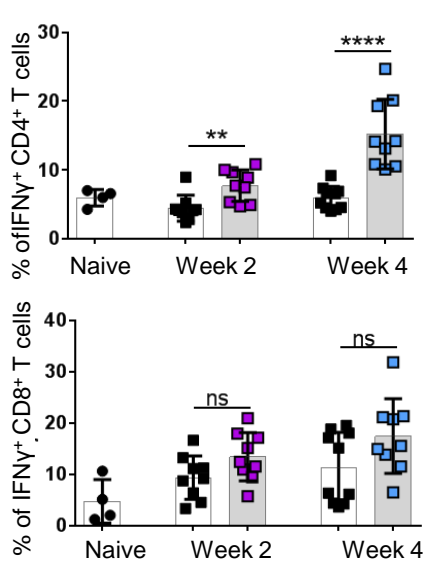
B



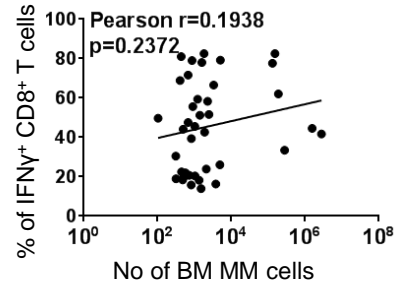
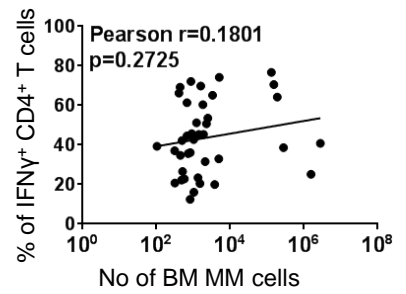
C



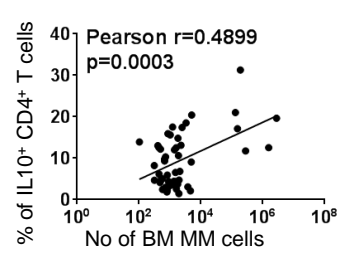
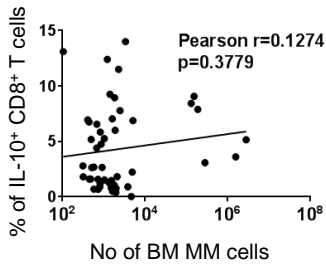
D



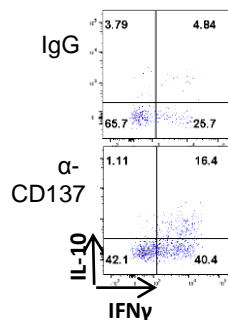
E



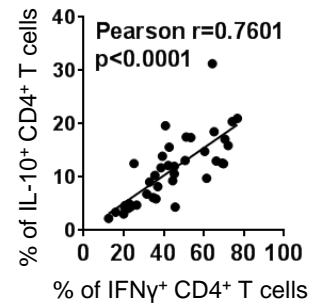
F



G

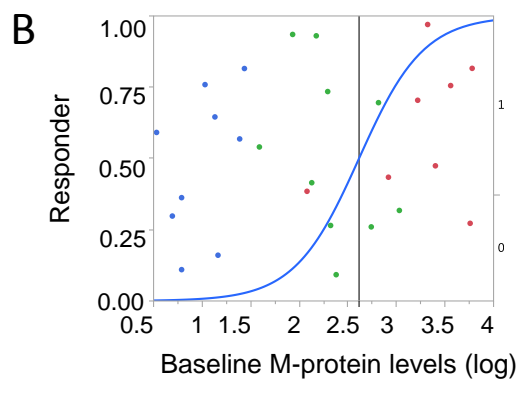
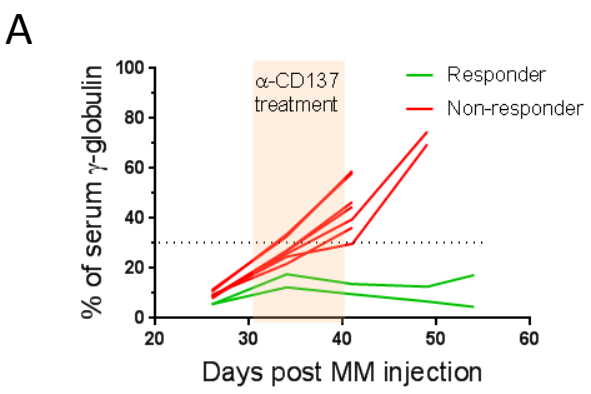


H



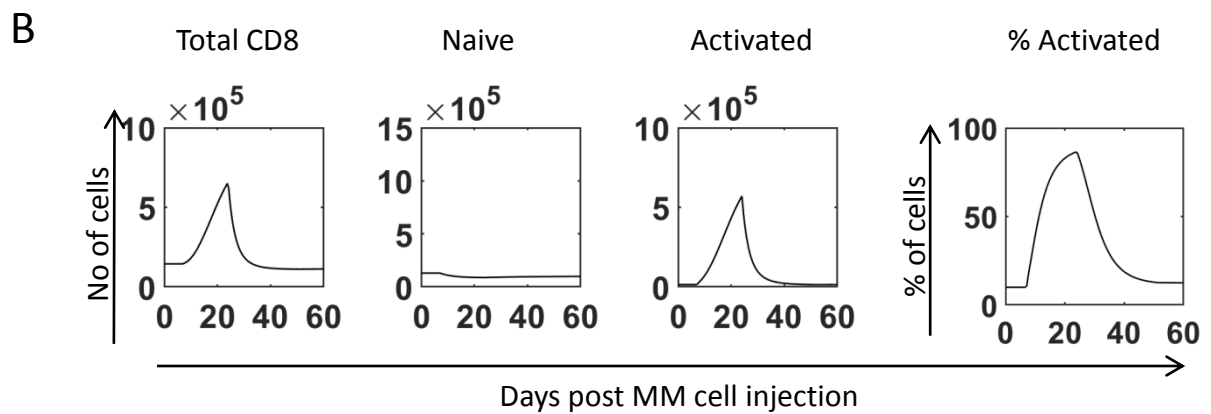
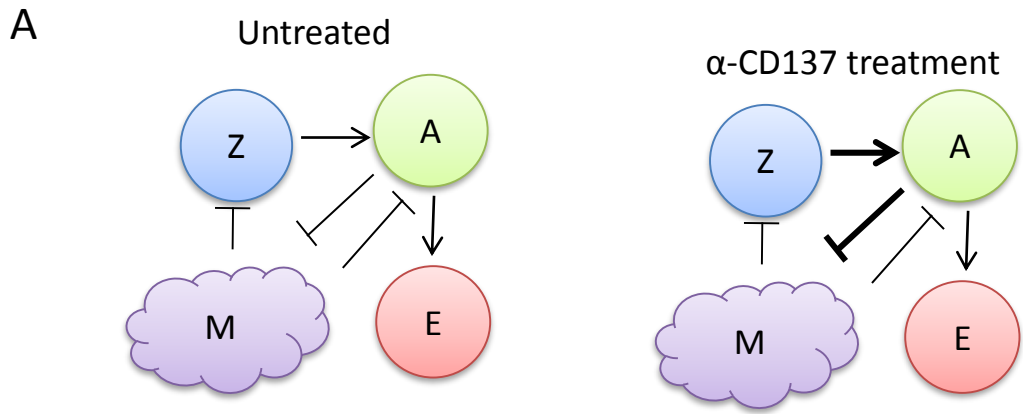
Supplemental Figure 6: The presence of high MM burden does not compromise T cell ability to produce IFN in response to CD137 stimulation. (A-D) WT mice received a single ip injection of 100 μ g of control IgG (black squares) or anti-CD137 mAbs (color squares) at week 2 or 4 post Vk*MYC cell challenge and NK cell- and T cell-responses were analyzed in the spleen 1 week later. (A) Representative dot-plot displaying NK cell percentages gated on spleen lymphocytes. (B) Quantification of spleen NK cell numbers. (C) Proliferation of FoxP3-CD4⁺ Th and CD8⁺ T cells was assessed by intracellular Ki67 staining. (D) BM cells were cultured with PMA-ionomycin for 2 hrs and IFN γ -production by CD4⁺ and CD8⁺ T cells was assessed by intracellular staining. Graphs show the (B) geometric mean \pm SD or (C,D) mean \pm SEM from 2 independent experiments with a total of n=6-10 mice per group. Data were analyzed using a Mann-Whitney U test, ** p < 0.01; *** p < 0.001; **** p < 0.0001; ns: non significant. (E-H) WT mice were challenged with Vk*MYC cells and 2-4 weeks later, mice received a 2-week anti-CD137 mAb treatment. At the end of the treatment, (E) IFN γ - or (F) IL10-production by BM CD4⁺ and CD8⁺ T cells was measured by intracellular staining. Data were pooled from n=5 independent experiments with n=50 anti-CD137 mAb-treated mice. Data were analyzed with a linear regression using log-transformed data for tumor burden. (G) Representative dot plot displaying co-staining for IFN γ and IL-10 on BM CD4⁺ T cells. (H) Correlation between the percentage of IFN γ ⁺ CD4⁺ T cells and IL-10⁺ CD4⁺ T cells, data were pooled from n=4 independent experiments with n=39 mice.

Supplemental Figure 7



Supplemental Figure 7: Mice can be divided into responders and non-responders to anti-CD137 mAb treatment. (A-B) WT mice were challenged with Vk^*MYC cells and 2-5 weeks later, serum M-protein levels were determined before and after mice received a 2 week anti-CD137 mAb treatment. Mice were categorized as responders if they were alive and their serum M-protein levels 2 weeks after treatment were below 30 %. (A) Example showing M-protein follow-up in an experiment with $n=7$ anti-CD137 mAb-treated mice. Responders are shown in green and non responders are shown in red. (B) Logistic fit model corresponding to Figure 7: Data from 3 independent experiments with a total of $n= 30$ mice are shown. Mice from a same experiment are displayed with the same color.

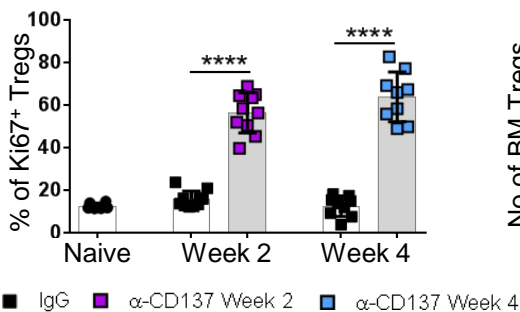
Supplemental Figure 8



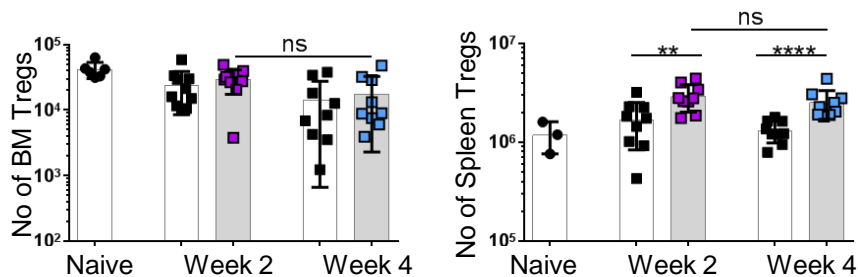
(A) Schematic representation of the interactions between the 4 populations: MM cells (M), naïve CD8⁺ T cells (Z), activated CD8⁺ T cells (A) and exhausted CD8⁺ T cells (E). Plain arrows represent conversions, \perp represent inhibitions. Naïve CD8⁺ T cells convert into activated CD8⁺ T cells that then convert into exhausted CD8⁺ T cells. Myeloma cells inhibit both naïve and activated CD8⁺ T cells and activated CD8⁺ T cells inhibit MM cells. Anti-CD137 mAb treatment further increases the conversion of naïve into activated CD8⁺ T cells and increases the inhibition of MM cells by activated CD8⁺ T cells. (B) The effect of a 2-week anti-CD137 mAb treatment on CD8⁺ T cell dynamic in the absence of tumor was modeled *in silico*. Treatment was started on day 7. Graphs show the numbers of total, naïve and activated CD8⁺ T cells as well as percentages of activated CD8⁺ T cells.

Supplemental Figure 9

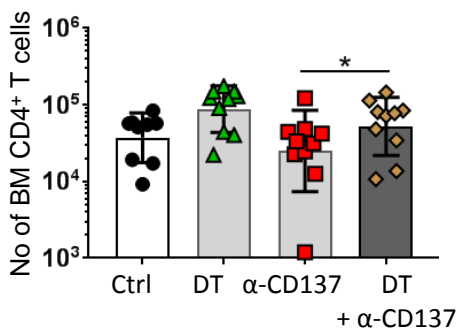
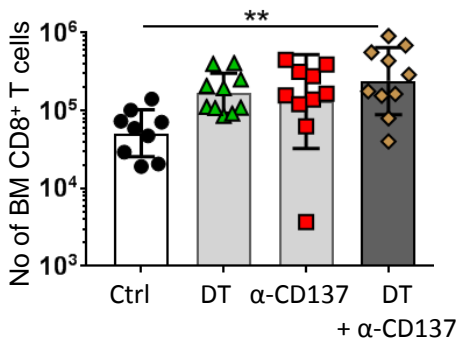
A



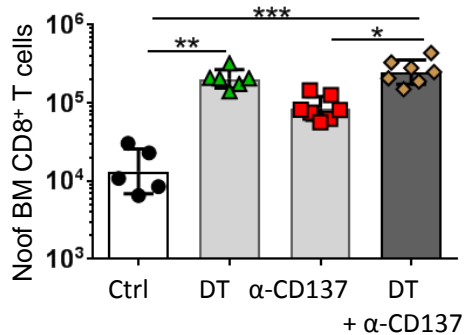
B



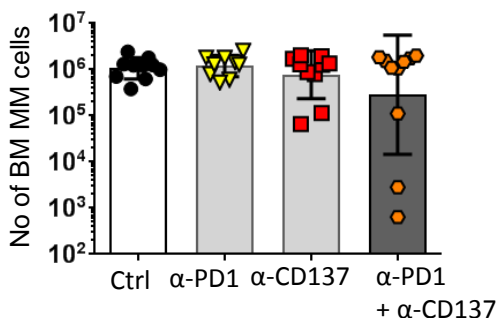
C



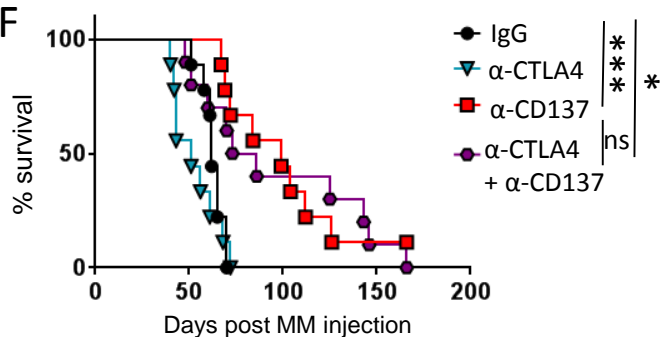
D



E



F

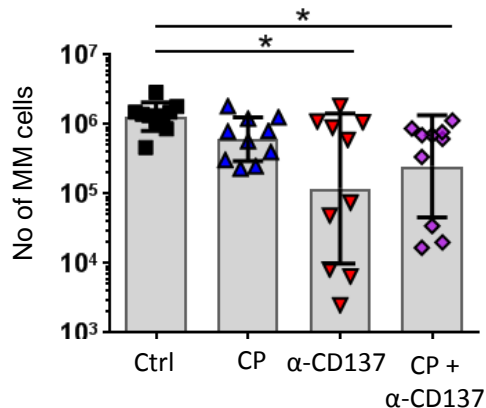


Supplemental Figure 9: Combination with anti-PD1 or anti-CTLA4 mAbs does not improve the efficacy of anti-CD137 mAb treatment.

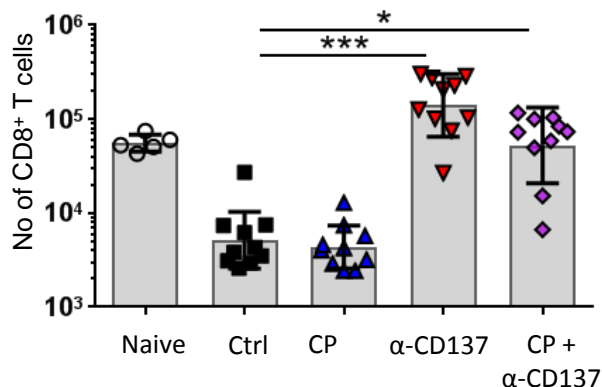
(A-B) WT mice received a single ip injection of 100 μ g of control IgG (black squares) or anti-CD137 mAbs (color squares) at week 2 or 4 post Vk*MYC cell challenge and 1 week later (A) proliferation of BM Tregs and (B) BM and spleen Treg numbers were determined by flow cytometry. (C) FoxP3-DTR mice challenged with Vk*MYC cells on day 0. Mice then receive an ip injection of 250 ng of diphtheria toxin (DT) (or PBS as control) on day 21 and 100 μ g of anti-CD137 mAbs (or control IgG) on day 22. BM T cells were analyzed by flow cytometry on day 28. (D) FoxP3-DTR mice were challenged with VK*MYC cells on day 0. Mice received 250 ng of DT on days 24 and 29, together with a 2-week anti-CD137 mAb treatment from day 25. CD8⁺ T cell numbers in the BM were analyzed on day 36. (E) WT mice were challenged with Vk*MYC cells and 3 weeks later, mice received an anti-CD137 mAb treatment combined with anti-PD1 mAbs. Numbers of MM cells in the BM were determined by flow cytometry at week 6 post Vk*MYC cell challenge. (A-E) Data are shown as mean \pm SEM (A) or geometric mean \pm SD (B-E) from (D,E) 1 experiment or (A-C) pooled from 2 independent experiments with n=5-10 mice per group. Data were analyzed with (A, B) a Mann-Whitney U test or (C-E) a Kruskal-Wallis test followed by a Dunn's multiple comparison post-hoc test. (F) WT mice were challenged with Vk*MYC cells and 3.5 weeks later mice received a 2 week anti-CD137 mAb treatment combined with anti-CTLA4 mAbs (mouse IgG2a, 200 μ l ip twice a week). Survival was followed over time. Data are from 1 experiment with n = 9-10 mice per group and were analyzed with a Log-Rank test. *p < 0.05; ** p < 0.01; *** p < 0.001; **** p < 0.0001; ns: non significant

Supplemental Figure 10

A

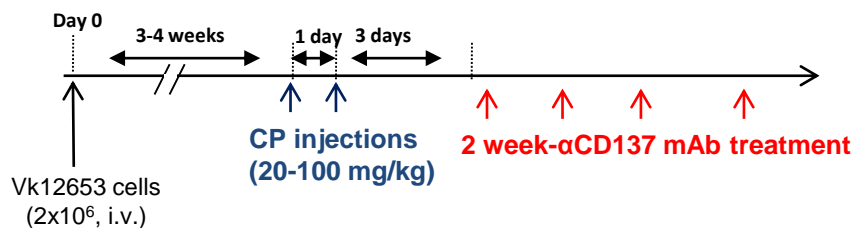


B

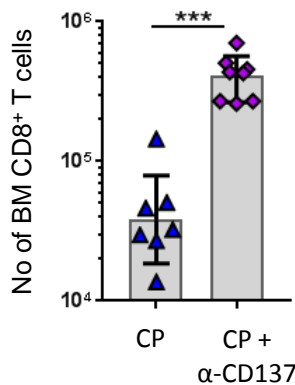


C

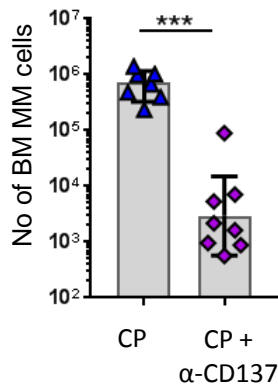
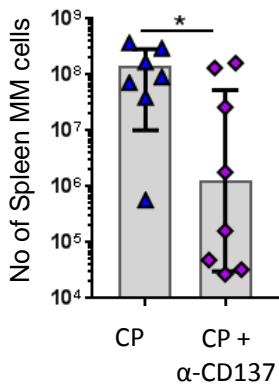
Sequential treatment



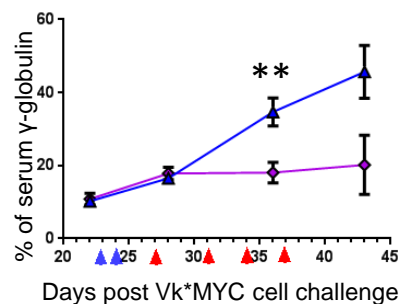
D



E



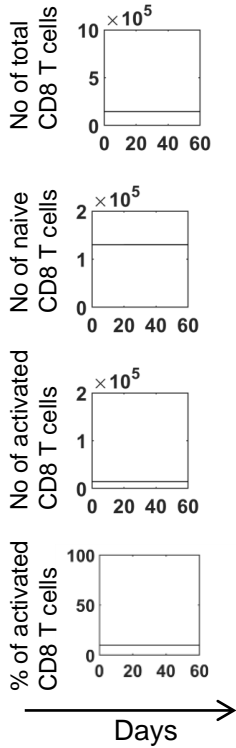
F



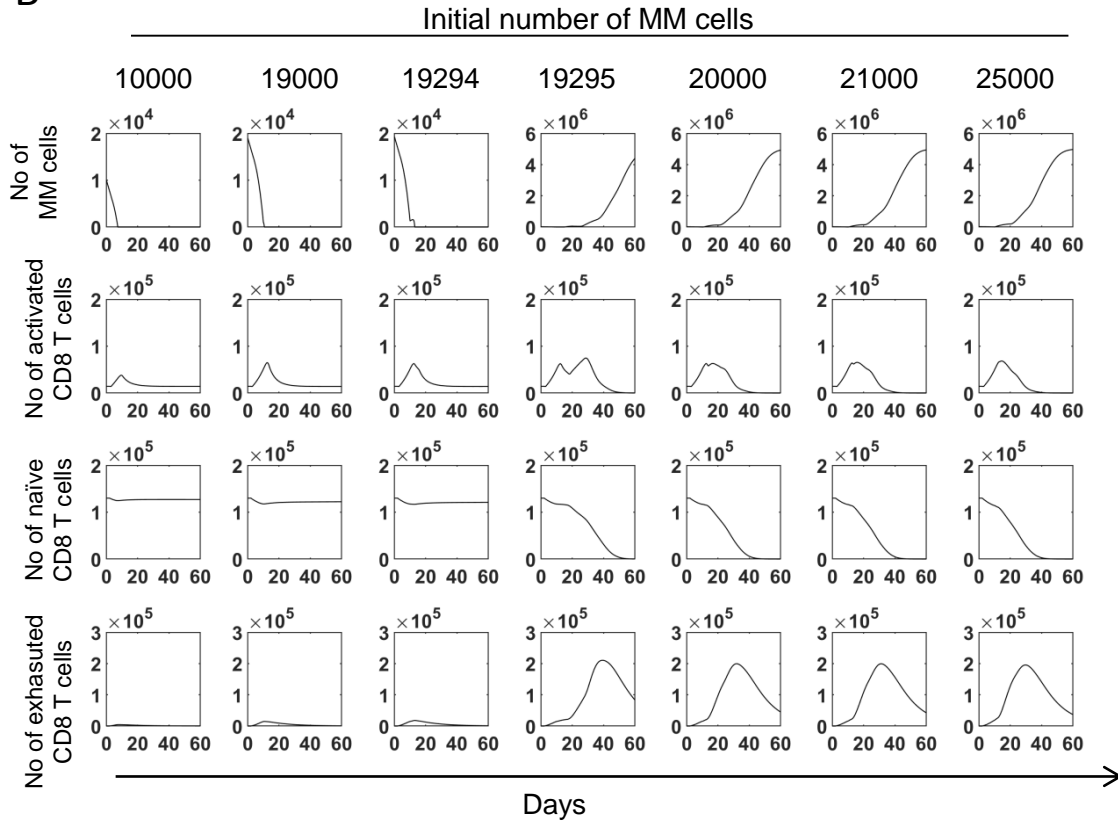
Supplemental Figure 10: (A-B) WT mice were challenged with $V\kappa^*MYC$ cells and 3 weeks later, mice received anti-CD137 mAb treatment combined with cyclophosphamide (CP) injections (20 mg/kg, twice a week). BM numbers of MM cells and CD8⁺ T cells were determined by flow cytometry at week 6 post $V\kappa^*MYC$ cell challenge. (C) Experimental design for sequential treatment with CP and anti-CD137 mAbs. Mice were given 2 injections of CP followed by a 2-week-anti-CD137 mAb-treatment. The time when the treatment was started and the doses of CP varied between experiments. (D-F) Mice received sequential treatment with CP and anti-CD137 mAbs as explained in (C). CP injections (25 mg/kg) were given on day 23 and 24. Flow cytometry analysis was performed on week 7. (D) Numbers of CD8⁺ T cells in the BM. (E) Numbers of MM cells in the spleen (left) and BM (right). (F) Serum M-protein levels overtime. Blue: CP + control IgG; purple: CP + anti-CD137 mAbs. Data are shown as (A, B, D, E) geometric mean \pm SD or (F) mean \pm SEM of 1 experiment with $n = 7-10$ mice per group. Data were analyzed using (A-B) a Kruskal-Wallis test followed by a Dunn's multiple comparison post-hoc test or (D-F) a Mann-Whitney U test. * $p < 0.05$, ** $p < 0.01$, *** $p < 0.001$.

Supplemental Figure 11

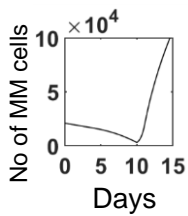
A



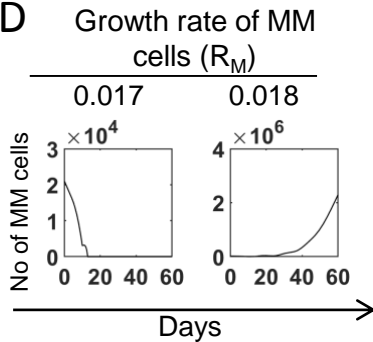
B



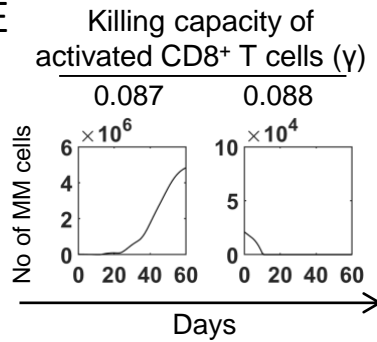
C



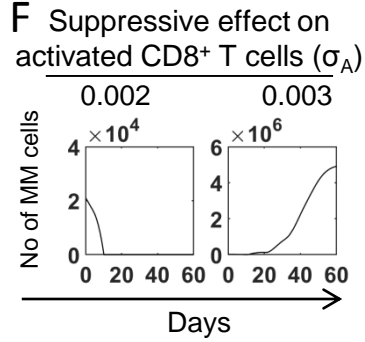
D



E



F



Supplemental Figure 11: Different simulation parameters determine the MM growth versus MM rejection outcome. Dynamic interactions between MM cells and CD8⁺ T cells were modeled *in silico*. (A) In the absence of tumor, numbers of naïve and activated CD8⁺ T cells remained constant, with activated CD8⁺ T cells representing 10 % of total CD8⁺ T cells. (B) Different initial numbers of tumor cells were tested while keeping the other parameters at their optimized values. Graphs show the numbers of MM cells as well as naïve, activated and exhausted CD8⁺ T cells overtime. (C) MM growth as per Figure 8A (21 000 initial MM cells), scale has been adjusted to visualize MM cell dynamics until day 15. (D) Numbers of MM cells overtime with limiting tumor growth rates ($R_M=0.017$ or $R_M=0.018$) while keeping the other parameters at their fitted values. (E) Numbers of MM cells overtime with increased activated CD8⁺ T cell killing capacity ($\gamma=0.087$ or $\gamma=0.088$) while keeping the other parameters at their fitted values. (F) Numbers of MM cells overtime with decreased tumor suppressive effect on activated CD8⁺ T cells ($\sigma_A=0.002$ or $\sigma_A=0.003$) while keeping the other parameters at their fitted values.